JOURNAL OF OPTOELECTRONICS AND ADVANCED MATERIALS, Vol. 9, No. 10, October 2007, p. 3021 - 3027

Invited Lecture

A new version of the RMC++ Reverse Monte Carlo programme, aimed at investigating the structure of covalent glasses

O. GEREBEN[a], P. JÓVÁRI[b], L. TEMLEITNER[b], L. PUSZTAI[b*]
[a]*Ardeus Ltd., H-2030 Érd, Fenyőfa u.32 Hungary*
[b]*Research Institute for Solid State Physics and Optics, Hungarian Academy of Sciences, H-1525 Budapest, P.O. Box 49, Hungary*

A new version of the RMC++ Reverse Monte Carlo (RMC) software, with major modifications and additions, is introduced. The capabilities of the code are demonstrated on the example of $Si_{40}As_{25}Te_{35}$ chalcogenide glass, for which simultaneous modelling of neutron and X-ray diffraction, as well as of (two sets of) EXAFS data is presented. By the extensive use of co-ordination constraints partial radial distribution functions (prdf) could successfully be separated.

(Received July 3, 2007; accepted October 1, 2007)

Keywords: Structural modelling, Reverse Monte Carlo, Covalent glasses

1. Introduction

The microscopic (atomic level) *structure* of a material is arguably its most basic property; the knowledge of it is essential for understanding (and/or evaluating) other properties, as well. The experimental technique that can provide direct information on the structure of a system in the condensed (solid and liquid) phases is (X-ray or neutron) *diffraction*.

For crystalline materials, in general, it is possible to determine the coordinates of each particle (atom or ion) in a 'building block' (unit cell) of the structure. For disordered (liquid and amorphous solid) systems, however, this is not possible, for the lack of such structural units; the description of the structure is only feasible in terms of *correlation functions* (see, e.g., Ref. [1]). As a further principal restriction, diffraction data, i.e. the most important experimental source of information, can uniquely characterise *pair correlations* only. In practice, diffraction data are always subject to limitations (most importantly, in terms of the scattering vector (Q-) range available) and errors (systematic and statistical); due to these, even the radial distribution function is burdened with (sometimes, significant) uncertainties (see, e.g., Refs. [2,3]).

The reasons for this deficiency of experiment-based knowledge are manyfold (multicomponent systems; presence of hydrogen; unfortunate combination of atomic scattering powers; etc...) but if one wants to name the origin of them then it can possibly be said that we simply want to derive far too many details on the grounds of measured quantities that are far too much of averaged in nature. The main consequence of all this is that there are many (sometimes, very) different local arrangements of neighbouring atoms/molecules that will result in the same two-particle correlation function - and we are able to measure only this latter (or rather, something related to this latter) directly. There is not much to improve on this sad situation (because we have no experimental means for that). However, one always has to bear this inherent feature in mind while dealing with structural features of disordered systems (and not to over-interpret results, either from experiment or modelling).

In what follows, we shortly describe a computational modelling tool, the so-called Reverse Monte Carlo (RMC) simulation, which has, over the past two decades, proven to be helpful in dealing with (but not solving!) the difficulties/uncertainties mentioned above. The main part of the paper is devoted to the description and demonstration of new features available in the latest version of the computer programme.

2. Reverse Monte Carlo modelling

Here, we would first like to describe shortly what RMC is and then, to emphasize properties which make it useful for interpreting diffraction and EXAFS results. For more detailed descriptions of the RMC method, see Refs. [4,5,6].

Reverse Monte Carlo is a simple tool for constructing large, 3D structural models that are consistent (within the estimated level of their errors) with the total scattering structure factors (tsf's) [7] obtained from diffraction experiments. Via random movements of particles, the difference (calculated similarly to the χ^2-statistics) between experimental and model total structure factors is minimised. From the particle configurations, the partial pair correlation functions, as well as other structural characteristics (neighbour distributions, cosine distribution of bond angles) can be calculated.

The Reverse Monte Carlo algorithm may be given as follows:

1. Start with an initial configuration with periodic boundary conditions. The positions of the N(>4000) atoms should be consistent with the molecular structure already at the start. Assume some tolerance for the intramolecular (bonded and non-bonded) disctances.

2. Calculate the partial pair distribution functions for this configuration

$$g_{ij}^{C,o}(r) = \frac{n_j^{C,o}(r)}{4\pi r^2 \Delta r \rho_j} \tag{1}$$

where $n_j^{C,o}$ is the number of atoms of type j at a distance between r and $r+\Delta r$ from a central atom of type i, averaged over all atoms of type i as centres. The superscripts C and o refer to 'calculated' and 'old', respectively. ρ_j is the number density of particles type j.

3. Compose the total pair distribution function(s) from the partials, weighted according to the concentrations and scattering powers of atoms:

$$G^{C,o}(r) = \sum_i \sum_j c_i c_j \overline{b_i}\,\overline{b_j}\left(g_{ij}(r) - 1\right) \tag{2}$$

where c's are molar fractions and b's are the (neutron) scattering lengths of the components. (Note that for X-rays, a more complicated way has to be followed since the X-ray scattering power of atoms depends on the scattering vector; for simplicity, throughout this contribution, the formalism of neutron scattering will be applied.) Transform to the total scattering structure factor

$$F^{C,o}(Q) - 1 = \frac{4\pi\rho}{Q}\int_0^\infty r G^{C,o}(r)\sin Qr dr \tag{3}$$

It is worthwhile remembering that in the RMC procedure, only transforms from r to Q space occur, which makes it easier to handle truncation errors, since the extent of the available r-range can be increased by using larger models.

4. Calculate the difference between the experimental total structure factor $F^E(Q)$ and that calculated from the configuration $F^C(Q)$

$$\chi_o^2 = \sum_k \frac{\left\{F^{C,o}(Q_k) - F^E(Q_k)\right\}^2}{\sigma^2} \tag{4}$$

where the sum is over all the experimental points and σ is the - estimated - experimental error, which functions as a 'control parameter' for the simulation. (By prescribing how close a fit to experiental data is required, σ controls the ratio of the numbers of accepted/attempted moves).

5. Move one atom at random.

6. Calculate the new pair distribution function, $G^{C,n}(r)$ and total structure factor, $S^{C,n}(Q)$, and the new difference between model and experiment, χ^2_n.

7. If $\chi^2_n < \chi^2_o$ the move is accepted and the new configuration becomes the old configuration. If $\chi^2_n > \chi^2_o$ then the move is accepted with probability $\exp\left\{-\left(\chi_n^2 - \chi_o^2\right)/2\right\}$.

8. Repeat from step 5.

In a 'normal' case (reliable data; meaningful input parameters), χ^2 will decrease until it reaches its minimum value, which minimum is linked to the given value of σ. After reaching its minimum (the state of 'structural equilibrium'), χ^2 will oscillate so that the ratio of the numbers of accepted/attempted moves will not decrease. If it does (and the run eventually would 'freeze in') then it is an indication that the structure formed is not the kind of 'global' minimum the algorithm is seeking. (For a demonstration of what an acceptable agreement between experimental and model structure factors is see Section 4 below.)

Over the years, RMC modelling helped us to understand a number of issues concerning structural disorder in general. Some of them are really obvious - so obvious that many times, we would be inclined to overlook them; let us list here some of these points, with - at least - references to more detailed descriptions.

(i) *There is always more than one structural model that would fit a given (set of) data -- and this has nothing to do with RMC!* RMC has just happened to be the technique which started to produce different models for a given data (see e.g. Refs. [8,9]), but it has to be recognised that it is the diffraction data that allow for diversity of models. Therefore, one must explore, as fully as (technically) possible, the 'configuration space' available for models connected to a (set of) measurement(s).

(ii) *In practice, there is always more than one (set of partial) pair correlation function(s) corresponding to a given (set of) tsf's.* This fact, demonstrated, for instance, in Refs. [3,10,11], is even less appreciated than the one under (i). There is no magic about it: this is just the consequence of the fact that there is no 'perfect data': your data will never span an infinite scattering vector range (which would be necessary for a perfect Fourier-transform) and your data will never be error-free, either (which would be a pre-requisite for a unique separation of the partials). That is, one has to consider more than one solution in terms of the pair correlation functions, as well.

(iii) One way of attempting to meet the above requirements is *the introduction of geometrical* (i.e., ones that can be formulated on the basis of the particle coordinates) *constraints*. These constraints can, for instance, represent specific ideas about the microscopic structure of the material in question; in this way, one will be able to tell if a given idea is consistent with existing measurements or not. That is, RMC can help us to select ideas/models which are (or are not) acceptable, on a very strict basis. This concept can be elaborated by using the new RMC++ software introduced here.

(iv) Modelling the structure factor with RMC will help to spot if there are problems (systematic errors) with that tsf (a clear demonstration of this feature can be seen in, for instance, Ref. [11]). Experience shows that if sensibly executed Reverse Monte Carlo runs do not lead to

a satisfactory agreement with tsf's then it is quite likely that it is the experimental structure factor that should be reconsidered (re-analysed; a little more theoretical approach to this problem can be found in Ref. [12]).

(v) As (at least, partly) a consequence of (ii), it should always be the total *structure factor* and not the (partial) radial distribution function(s) that are applied as input data for RMC. First of all, tsf's constitute the primary experimental information whereas (p)rdf's will always contain errors related to the the direct Fourier transform from reciprocal to real space. Additionally, a given (set of partial) rdf('s) has to be considered only as one (out of the many possible) interpretation of the tsf('s). Thus, modelling only one (set of partial) rdf('s) will certainly be insufficient for a proper coverage of possible structures that are consistent with the experimental data in question.

3. New features of the RMC++ software: a technical description

The RMC++ code [6] (written by Guillaume Evrard [6]) was used as the starting point for the present development. Our primary aim was to add new features and, if possible, to increase speed. To perform this task efficiently, first the programme was partially redesigned to make its structure clearer and more genuinely object oriented, via replacing most of the numerous object independent routines by member routines of the proper objects.

Secondly, there is no need anymore to use different source files for different platforms (connected mostly to the platform-dependent file handling); the same source code can be used (tested so far on Linux, Windows and Macintosh). Some option switches governing the custom-made building of the executable were introduced to make the code faster by leaving out unnecessary parts, or in case of ATLAS [13] usage, to be described below, to make it possible to compile and run the code without the ATLAS libraries.

Due to the new features introduced, the structure of the **.dat* file containing the parameters of the run has changed slightly. The main changes compared to the starting RMC++ and the added new features will be described briefly below.

3.1. Changes made as compared to the previous version of RMC++

a) The possibility to model EXAFS data was included.

b) The coordination number constraint was generalized, so now not only one, but also a specified number of neighbour types can be constrained. For example, in case of 3 atom types it is possible to define a constraint that the central atom of $type_1$ should have 3 atoms belonging to $type_2$ and $type_3$ in the distance ranges $r_{min}[type_2] \rightarrow r_{max}[type_2]$ and $r_{min}[type_3] \rightarrow r_{max}[type_3]$, respectively; this means that there are several possibilities satisfying this constraint ($type_2$-$type_2$-$type_2$, $type_2$-$type_2$-$type_3$, $type_2$-$type_3$-$type_3$ and $type_3$-$type_3$-$type_3$). Such a construction is extremely useful for covalent glasses where the valences of the constituents are known but the identity of the possible neighbours are not.

c) New constraint for the cosine distribution of bond angles was included. The calculation method for the theoretical distribution can be either a step function or a Gaussian. Step function means having uniform distribution with integral 1 for a range of angles (zero otherwise). Gaussian indicates a normal distribution with integral 1 having the maximum at the specified angle, with a specified width.

d) The possibility of the swaps of different type particles was included. The swap fraction (fraction of swaps related to the generated moves) is the parameter controlling the frequency of the swaps (has to be between 0 and 1) is included into the *.dat file* followed by for each mixed partial a Boolean indicator 1 (if the given partial can be involved in swap) or 0 (not involved in swap) controlling what kind of swaps can be performed. Swaps can be used only in case of atomic (even multi-atomic) moves, but not with the FNC option. Obviously cannot be used in case of a mono-atomic system.

e) The partial radial distribution function(s), *prdf* can be optionally collected at each saving, and the average prdf('s) is(/are) calculated and saved, too.

f) A new class (NeighbourList) for the gridding of the simulation box and for the neighbour list was created. A new parameter, giving the desired number of particles in a grid cell can be found in the **.dat* file. Based on this, the average number density of the sample and an additional safety parameter, the program determines the number of grid cells. The gridding is used for a preliminary check, whether the cutoff distances are satisfied before entering the lengthy calculation of the change in the histogram. For this only the information provided by the gridding is used, whereas the neighbour list is not. If there is/are constraint(s) for the cosine distribution of bond angles then the neighbour lists are created for the constrained types only. As the program was designed to be as quick as possible and as nowadays the size of the computer memory does not pose any serious limitation, not only the indices of the neighbours but also their type, squared distance from their central atom and the components of the central→neighbour vector are stored, thus sparing computational time. During the simulation loop the gridding and the neighbour list (if it exists) are not recalculated completely, but only updated for the atoms affected by the move to make the simulation faster.

g) The possibility to achieve some additional speed increase with the usage of the Automatically Tuned Linear Algebra Software (ATLAS) [13] for matrix-vector multiplication was included. The libraries have to be installed separately, so only use this option if these libraries are available! The installed ATLAS libraries are using the BLAS routines, optimised for the given platform, and can increase the speed of the vector-vector, matrix-vector and matrix-matrix operations. In RMC, ATLAS is exploited for the Fourier-transformation of (neutron-weighted) *S(Q)* and (X-ray-weighted) *F(Q)* (matrix-vector multiplication).

The programme (including the source code), a more detailed description and an example run are available at the web site www.szfki.hu/~nphys/rmc++/opening.html.

3.2. Parallelisation, speed comparison

The new code is available in two versions: one is the standard, consecutive RMC++_new and the other is a multi-threaded version (RMC++_multi) written for shared memory multi-processor computers, using the Portable Operating System Interface (POSIX) thread standard, to increase the speed of the calculation by distributing the work between the threads. POSIX is natively UNIX-LINUX based, but there is a freely available interface, POSIX for Win32, which makes it easy to run the program under WINDOWS. The functionality of this version is the same as of the standard, consecutive version. The only difference in the usage is that the total number of threads (recommended to match the number of available processors) has to be specified in the **.dat* file. For the thread-specific tasks, a new class 'Thread' was introduced.

During the RMC simulation, distances between particles are calculated at least up to half the box length to give good statistics and make the pair correlation function decay to minimize truncation errors during Fourier transformation. This long-range correlation made parallelisation by spatial decomposition impossible. As the entire course of the RMC simulation (except the optional final, configuration collecting phase) can be compared to the warm-up period of a Monte Carlo (MC) simulation, time decomposition by running independent, parallel simulations differing only in the random number seed was equally unsuitable.

Parallelisation could finally be achieved by using an unmodified Markov chain with a 'farm algorithm' [14], simply distributing the most time-consuming calculation steps among the processors. All the threads of the programme share the memory and the data segment. The main thread takes care of the non-parallelised work, creates the auxiliary threads, makes the move(s) and splits the tasks among the threads while taking an equal share in the calculation, as well. The auxiliary threads exist for the whole duration of the program and execute tasks when they receive signal from the main thread. Parallelisation is used during calculating the histogram and its change, the *prdf*, the initial and modified partial and *total g(r), S(Q), F(Q)* and *E(Q)* calculation and the copying of the changed histogram, *prdf* and partial parts after acceptance/rejection was decided.

Even if the newly added features are not used, it is recommended to use the new version, as even without the speed increase provided by ATLAS and/or multi-threading RMC++_new proved to be 1.5 times quicker than RMC++ on our test system. The speed increase caused by ATLAS and/or multi-threading depends on the actual parameters of the simulation (number of atoms, number of histogram bins, number and size of the experimental data, number of available processors), so no general answer can be given. Several tests were performed on various platforms with varying system sizes. ATLAS usage increased the speed by a factor of 1.9-2.6 for RMC++_new and 1.2-1.9 for 2-threaded RMC++_multi. For the comparison of the standard and the multi-threaded versions, performance efficiency [15] is used: $E(p)=\frac{S(1)}{S(p)p}100\%$, where p is the number of processors and $S(1)$ and $S(p)$ are the elapsed times for the single-threaded standard and for the p-threaded applications, respectively. The speed increase of RMC++_multi over RMC++_new is about $E(2)$=93-99% without ATLAS and $E(2)$=51-81% with ATLAS.

Based on the findings of these tests, we suggest that it is worth using either standard RMC++_new with ATLAS, or with multi-threading; in most of the cases the combined ATLAS/multi-threading version proves to be best. However, it is a good idea to check, especially before a long simulation, which code is giving the best performance for your system on the given platform.

4. A test case: amorphous $Si_{40}As_{25}Te_{35}$

Studying the microscopic structure of ternary amorphous alloys is a rather demanding task. In some favourable cases (especially if there are large size differences and/or strong bonding preferences between constituents) satisfactory structural information can be collected from only 2 or 3 (diffraction and/or EXAFS) measurements. However, in general, the 6 partial radial distribution functions can be separated only by combining X-ray, neutron diffraction and two or three EXAFS datasets. The merit of these techniques has already been dicussed in detail elsewhere [16,17]. Here we only mention that by combining these techniques in most cases we can obtain relatively precise coordination numbers (due to diffraction) and relatively accurate nearest neighbour distances (due to EXAFS). Exceptions can be alloys of elements with similar neutron scattering lengths and close electron numbers (e.g. Ga-Se, As-Se, Ge-Se, Sb-Te), which are thus indistinguishable for X-ray photons, neutrons and for photoelectrons, as well.

In this session we demonstrate the capabilities of the new version of RMC++ by applying it to glassy $Si_{40}As_{25}Te_{35}$. For experimental details we refer to a previous structural study on this alloy [17]. Simulations were started from an initial configuration containing 4000 atoms. The number density was 0.03365 $Å^{-3}$. The initial configuration satisfied the following cut-off criteria: r_{AsAs} = 2.2 Å, r_{AsTe} = 2.4 Å, r_{AsSi} = 2.1 Å, r_{SiSi} = 2.2 Å, r_{SiTe} = 2.3 Å. As a previous Raman measurement strongly suggests [18] that there is no significant Te-Te bonding in this alloy the Te-Te cut off was set to 3.1 Å.

In the first step we fitted simultaneously the X-ray and neutron diffraction datasets. Coordination numbers and bond lenghts are listed in Table 1. It can be observed that

the Si-Si, Si-As and As-As distances are quite close to each other. The similarity of the average number of neighbours of As and Si (noted by As-X and Si-X) also suggests that As and Si cannot be distinguished if only the two diffraction measurements are modelled.

Table 1. Nearest neighbour distances r_{ij} and coordination numbers N_{ij} for amorphous $Si_{40}As_{25}Te_{35}$, fitting ND and XRD data only.

Pairs	Si-Si	Si-As	Si-Te	As-Si	As-As	As-Te	Te-Si	Te-As	Si-X	As-X	Te-X
r_{ij} (Å)	2.36	2.34	2.50	2.34	2.39	2.55	2.50	2.55	–	–	–
N_{ij}	1.27	1.21	1.13	1.93	1.18	0.45	1.29	0.32	3.61	3.56	1.61

The situation can be improved by including Si- and As K-edge EXAFS data in the modelling. A great advantage of EXAFS is its element sensitivity, which means two things. First, by selecting an absorption edge we can obtain information specific to the environment of the absorbing species. Second, the amplitude and phase of backscattered photoelectrons depends on the type of backscatterer (neighbour). In favourable situations the latter makes it possible to observ correlations between minority components. For example the existence of Ge-Sb bonds in amorphous $Ge_2Sb_2Te_5$ was shown by fitting diffraction and EXAFS data with and without Sb-Ge pairs [16]. Ge and Te possess strongly different photoelectron backscattering properties thus the absence of Ge neighbours resulted in the worsening of the fit of Sb K-edge measurement. On the other hand, due to the similar back-scattering power of Sb and Te Ge-Sb bonding had no effect on the fit of Ge K-edge data.

Table 2. The nearest neighbour distances r_{ij} and coordination numbers N_{ij} for amorphous $As_{25}Si_{40}Te_{35}$, fitting 4 measurements.

Pairs	Si-Si	Si-As	Si-Te	As-Si	As-As	As-Te	Te-Si	Te-As	Si-X	As-X	Te-X
r_{ij} (Å)	2.37	2.36	2.49	2.36	2.44	2.56	2.49	2.56	–	–	–
N_{ij}	1.23	1.39	1.04	2.22	1.15	0.38	1.19	0.27	3.66	3.75	1.46

Results obtained by fitting the 4 measurements simultaneously are summarized in Table 2. Due to the information in As K-edge data the difference between Si-As and As-As distances increased to 0.08 Å. But it can also be observed that the Si-Si bond length became longer than the Si-As one. As we have no Si K-edge data and Si is a relatively weak scatterer both for photons and neutrons the uncertainty of the Si-Si distance is relatively large. While obtaining more reliable distances, the reliability of coordination numbers have not been improved by adding As and Te K-edge data. The average coordination number of As became greater than that of Si showing that the artificial mixing of As and Si is only partly resolved.

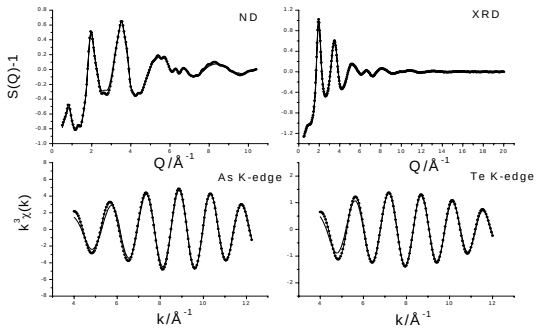

Fig. 1. XRD and ND structure factors, and EXAFS spectra for $Si_{40}As_{25}Te_{35}$ glass. Circles – measured. Lines – obtained by simultaneous RMC simulation of the experimental XRD, ND and EXAFS data, with constraints added (see text).

In the next step some coordination constraints were introduced. In line with basic inorganic chemistry (which is supposed to be valid for this alloy) we assumed that *every* Si, As and Te atom has exactly 4, 3 and 2 neighbours, respectively. The type of the neighbours was not constrained, only the maximum distances, which were equal to the minimum of the corresponding partial radial distribution functions obtained from the preceding unconstrained runs. Note that these constraints are much stronger than setting the *average* coordination number of Si to 4 etc. The constraints were satisfied for more than 90% of the atoms. The RMC fits obtained are shown in Figure 1, while coordination numbers and bond lengths are listed in Table 3. The difference between Si-Si and As-As bond lengths increased from 0.07 Å to 0.12 Å. A smaller but significant increase can be observed for the difference of As-Te and Si-Te bond lengths. All these suggest that by constraining the coordination numbers the degeneracy of As and Si is resolved. It can be observed that the number of homopolar Si-Si and As-As bonds is rather high. A significant As-As bonding was also found in Ag- doped As_2Te_3 [19]. Coordination number values also suggest that As-Si and Te-Si bonds are preferred to As-Te ones. Thus by combining 4 datasets and using some constraints the 6 partial pair correlation functions could be separated. It should be mentioned that the neutron data range is rather limited and none of the synchrotron measurements (high energy XRD and EXAFS) took more than 2 hours. This approach has already been succesfully applied to Ag- and I-doped As_2Se_3, as well [20,21].

Table 3. The nearest neighbour distances r_{ij} and coordination numbers N_{ij} for amorphous $As_{25}Si_{40}Te_{35}$, fitting 4 measurements and using constraints.

Pairs	Si-Si	Si-As	Si-Te	As-Si	As-As	As-Te	Te-Si	Te-As	Si-X	As-X	Te-X
r_{ij} (Å)	2.32	2.36	2.48	2.36	2.44	2.58	2.48	2.58	–	–	–
N_{ij}	1.81	1.02	1.27	1.63	0.77	0.63	1.45	0.45	4.10	3.03	1.90

Partial radial distribution functions, resulting from this last set of calculations, are shown in Figure 2. Small spikes can be observed on the As-Si, As-Te and Si-Te prdf's. These are either from the coordination constraints (e.g. the imposed constraints can be satisfied only by increasing artificially the intensity on one or two bins) or from EXAFS. Experience shows that such spikes – or in some cases even 'side wings' – can often be found in models fitting EXAFS data. These features may appear if they improve the fit of EXAFS data and the weight of the corresponding partial pair correlation function is low in other measurements.

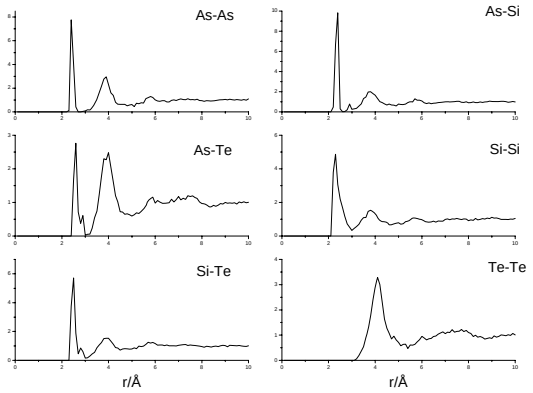

Fig. 2. Partial radial distribution functions for $Si_{40}As_{25}Te_{35}$.

There is no general solution to eliminate them but some simple 'rules' may often help. For example, the magnitude of the spurious features is usually smaller if $k^n\chi(k)$ (n=2,3) is fitted, instead of $\chi(k)$. The real space range used to fit $\chi(k)$ is also important. Distant shells have rather low contribution to the EXAFS signal, which means that small oscillations at higher r values can be magnified without significantly influencing the quality of the fit. This is the reason why it is in most cases better to fit the filtered data (the backtransformed first shell of the Fourier transform of $k^n\chi(k)$) instead of raw experimental $\chi(k)$ and restrict the fitting range only to the first shell distances. Such filtering can be carried out by any of the different EXAFS visualizing and analyzing programs e.g. Viper [22] or Athena [23]. More interested readers may also have a look at the ESRF EXAFS package pool [24]. If everything fails then it may still be possible to decrease the value of the partial pair correlation function over the suspicious bins by using an additional coordination constraint. Though this solution seems to be symptomatic, the new version of RMC++ offers a rather quantitative tool to judge whether such a feature is significant or not. One of the several useful outputs is the *.peq* file that contains the EXAFS analogon of partial structure factors, the *k*-space signal from the g(r) functions contributing to the model EXAFS curve (e.g. g_{AsAs}, g_{AsSi} and g_{AsTe} for As K-edge). Thus it is possible to check whether the contribution of a spike is significant in *k*-space as well. In many cases spectacular r-space features have only a minor influence on the model EXAFS signal, which suggests that they are most likely simulation artefacts.

5. Conclusions

The new, largely extended and re-structured Reverse Monte Carlo code, RMC++_new (and its different parallel versions) has been introduced. It has been shown that the software in its present form is extremely useful for modelling the structure of covalent glasses.

Acknowledgments

We thank Dr. Mikael Leetma (Stockholm University, Sweden) for drawing our attention to the ATLAS package. This work has been supported by the Hungarian Basic Research Fund 'OTKA' (Grant No. T048580).

References

[1] J.-P. Hansen, I.R. McDonald, *The Theory of Simple Liquids,* Academic Press, London (1986).
[2] L. Pusztai, R.L. McGreevy, J. Neutron Research **8**, 17 (1999).
[3] L. Pusztai, R.L. McGreevy, J. Phys.: Cond. Matter **10**, 525 (1998).
[4] R.L. McGreevy, L. Pusztai, Molec. Simul. **1**, 359 (1988).
[5] R.L. McGreevy, J. Phys.: Cond. Matter **13**, R877 (2001); L. Pusztai, J. Non-Cryst. Sol. **227-230**, 88 (1998).
[6] G. Evrard, L. Pusztai, J. Phys.: Cond. Matter. **17**, S1 (2005).
[7] D.A. Keen, J. Appl. Cryst. 34, 172 (2001).
[8] M.A. Howe, R.L. McGreevy, Phys. Chem. Liq. **24**, 1 (1991).
[9] O. Gereben, O., L. Pusztai, Phys. Rev. B, **50**, 14136 (1994).
[10] L. Pusztai, Phys. Rev. B **60,** 11851 (1999).
[11] L. Pusztai, Phys. Rev. B **61,** 28 (2000).
[12] L. Pusztai, O. Gereben, A. Baranyai, Physica Scripta **T57**, 69 (1994).

[13] R.C. Whaley, A. Petitet, J.J. Dongarra, Parallel Computing **27**, 3 (2001).
[14] S.J. Zara, D. Nicholson, Molecular Simulation **5,** 245 (1990).
[15] G.S. Heffelfinger, Comput. Phys. Commun. **128,** 219 (2000).
[16] P. Jóvári, I. Kaban, J. Steiner, B. Beuneu, A. Schöps, A. Webb, J. Phys.: Cond. Matter **19**, 335212 (2007).
[17] I. Kaban, S. Gruner, P. Jóvári, M. Kehr, W. Hoyer, R.G. Delaplane, M. Popescu, J. Phys.: Cond. Matter **19**, 335210 (2007).
[18] A. Lörinczi, F. Sava, M. Iovu, M. Leonovici, Th. Halm, M. Popescu, W. Hoyer, Phys. Stat. Sol. (b) **240,** 29 (2003).
[19] I. Kaban, P. Jóvári, W. Hoyer, I. Lishchinkii, T. Petkova, P. Petkov, unpublished results (2007).
[20] I. Kaban, W. Hoyer, T. Petkova, P. Petkov, B. Beuneu, A. Schöps, M. A. Webb, J. Ovonic Research **3**, 67 (2007).
[21] I. Kaban, W. Hoyer, T. Petkova, P. Petkov, B. Beuneu, A. Schöps, M.A. Webb, J. Optoelectron. Adv. Mater. **9**, 2750 (2007).
[22] K.V. Klementev, J. Phys.D: Appl.Phys. **34** 209 (2001); see also www.desy.de/~klmn/viper.html
[23] http://cars9.uchicago.edu/~ravel/software/
[24] http://www.esrf.eu/computing/scientific/exafs/

*Corresponding author: ep@szfki.hu